Heavy-to-heavy quark decays at next-to-next-to-leading order

Alexey Pak and Andrzej Czarnecki

Department of Physics, University of Alberta, Edmonton, Alberta, T6G 2G7, Canada

(Received 20 August 2008; published 11 December 2008)

Details of a recent calculation of $\mathcal{O}(\alpha_s^2)$ corrections to the decay $b \to c\ell\nu_l$, taking into account the c-quark mass, are described. Construction of the expansion in the mass ratio m_c/m_b as well as the evaluation of new four-loop master integrals are presented. The same techniques are applicable to the muon decay, $\mu \to e\nu_\mu\bar{\nu}_e$. Analytical results are presented, for the physical cases as well as for a model with purely-vector couplings.

DOI: 10.1103/PhysRevD.78.114015 PACS numbers: 12.38.Bx, 13.20.−v

I. INTRODUCTION

Because of the role that the semileptonic decay $b \to c\ell\nu_l$ and the muon decay $\mu \to e\nu_\mu\bar{\nu}_e$ play in the determination of the parameters of the standard model, it is warranted to improve the theoretical description of their rates and distributions. Recently, we have determined $\mathcal{O}(\alpha_s^2)$ corrections (α^2 for the muon), including the effects of the charm quark (electron) mass [1]. Since this was the first analytical evaluation of such mass effects and required an extension of known results, in this paper we describe some technical details.

We made extensive use of earlier results obtained in the massless case [2–4], in particular, of the master integrals determined in those projects. It turned out, however, that the massive case requires the knowledge of more terms of the expansion of those integrals in the dimensional regularization parameter $\epsilon = \frac{4-D}{2}$. To find them, we took a different approach to the evaluation of those master integrals. That approach is described below, together with the list of new terms that are now known. Since the decays considered here are a model for other beta-decaylike processes, those integrals will likely find other applications in the future.

Before presenting that calculation, in the following section we introduce the notation and in Sec. III we describe how the expansion around the massless case is constructed. Our results for the corrections to the $b \to c$ decay and to a decay in a model with pure vector couplings, as well as for the new terms in master integrals, are collected in three appendices.

II. DECAY RATE AND RADIATIVE CORRECTIONS

The tree-level decay rate and the one-loop corrections are known exactly [5]. Their expansion in $\rho \equiv m_c/m_b \ll 1$ and parametrization of two-loop corrections are

$$\Gamma(b \to c\ell\bar{\nu}) = \Gamma_0\left[X_0 + C_F\frac{\alpha_s(m_b)}{\pi}X_1 + C_F\left(\frac{\alpha_s(m_b)}{\pi}\right)^2 X_2 + \ldots\right], \tag{1}$$

$$X_0 = 1 - 8\rho^2 - 24\rho^4\ln\rho + 8\rho^6 - \rho^8, \tag{2}$$

$$\begin{aligned} X_1 = {} & \frac{25}{8} - \frac{\pi^2}{2} - (34 + 24\ln\rho)\rho^2 + 16\pi^2\rho^3 \\ & - \left(\frac{273}{2} - 36\ln\rho + 72\ln^2\rho + 8\pi^2\right)\rho^4 + 16\pi^2\rho^5 \\ & - \left(\frac{526}{9} - \frac{152}{3}\ln\rho\right)\rho^6 + \ldots, \end{aligned} \tag{3}$$

$$\begin{aligned} X_2 = {} & T_R N_L X_L + T_R N_H X_H + T_R N_C X_C + C_F X_A \\ & + C_A X_{NA}, \end{aligned} \tag{4}$$

where $\Gamma_0 = G_F^2|V_{cb}|^2 m_b^5/(192\pi^3)$, G_F is Fermi constant, and color factors are $C_F = \frac{4}{3}$, $T_R = \frac{1}{2}$, $C_A = 3$. Here $N_L = 3$ is the number of massless quarks, and $N_{H,C} = 1$ label, respectively, the b-quark loop, and virtual and additional real c-quark contributions; components X_L, X_H, X_C, X_A, and X_{NA} are separately gauge-invariant and finite. The limit of these functions for $m_c = 0$ is known [3]. The purpose of this paper is to obtain their mass dependence. All calculations are performed in $D = 4 - 2\epsilon$ dimensions, and axial currents are treated according to the prescription of [6]. General gluon gauge was used to ensure gauge invariance of the results.

The presence of the logarithm of the mass ratio in the lowest-order rate, Eq. (2), signals the presence of higher powers of logarithms in the higher-order terms [indeed, we see a quadratic logarithm in Eq. (3)]. It is for this reason that the term ρ^4 requires more terms of the expansion of Feynman integrals in powers of ϵ mentioned in Sec. I.

Using the optical theorem, we find X_2 as the imaginary part of 39 self-energy diagrams such as the examples shown in Fig. 1. Each diagram is expanded in asymptotic regions [7–9] to several orders in ρ and all contributions are summed. Some details of that expansion are described in the next section.

III. ASYMPTOTIC EXPANSION

As an example, we consider the rightmost diagram in Fig. 1 which has the richest structure of asymptotic re-

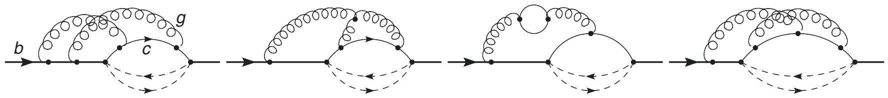

FIG. 1. Examples of $\mathcal{O}(\alpha_s^2)$ b-quark self-energy diagrams whose cuts describe the semileptonic decay. Dashed lines represent a charged lepton and a neutrino, whose masses we neglect.

gions. Evaluating the traces and Wick rotating, we obtain a number of terms proportional to integrals

$$\begin{aligned}
&\int \frac{d^D k d^D q d^D r d^D l}{D_1^{a_1} \ldots D_9^{a_9}}, \qquad D_1 = k^2, \\
&D_2 = (q-r)^2 + m_c^2, \qquad D_3 = q^2 + m_c^2, \\
&D_4 = (q+l)^2 + m_c^2, \qquad D_5 = (q+l-r)^2 + m_c^2, \\
&D_6 = r^2, \qquad D_7 = l^2, \qquad D_8 = l^2 + 2pl, \\
&D_9 = (p+k-q+r)^2,
\end{aligned} \tag{5}$$

(Fig. 2(a)), where the external momentum p is on shell ($p^2 = -m_b^2$), and exponents a_i are some integers. To reduce the problem to single-scale integrals, we investigate all possible assignments of the two relevant scales—m_b (“hard”) or m_c (“soft”)—to the four-loop momenta, and Taylor expand in every such “region” (Figs. 2(b)–2(l)).

As an example, consider q and l being soft, and k and r hard. The denominators are Taylor expanded as

$$\begin{aligned}
&\frac{1}{D_8} = \frac{1}{l^2 + 2pl} = \frac{1}{2pl} \sum_{i=0}^{\infty} \left(-\frac{l^2}{2pl} \right)^i, \\
&\text{and similarly } \frac{1}{D_2} \to \sum_i \frac{\ldots}{D_6^i}, \\
&\frac{1}{D_5} \to \sum_i \frac{\ldots}{D_6^i}, \qquad \frac{1}{D_9} \to \sum_i \frac{\ldots}{[(p+k+r)^2]^i},
\end{aligned} \tag{6}$$

producing, together with the remaining denominators, case (i). Similar expansions in the other regions are summarized in Table I.

As one can see, in most regions this topology factorizes into known one- and two-loop integrals. Note the unusual “eikonal” denominators such as $1/(2pl + i0)$ in cases (i) and (l), which lead to odd powers of ρ in the end result.

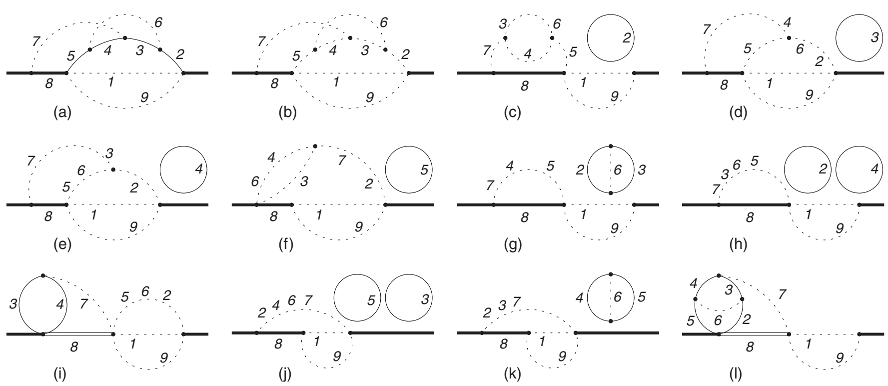

FIG. 2. Expansion of a double-scale topology (a) in all contributing asymptotic regions (b–l). Thick lines represent mass m_b, thin lines represent mass m_c, dashed lines are massless, double lines correspond to eikonal (static) propagators. Different regions correspond to expansions with different assignment of scales (hard, m_b or soft, m_c) to the four-loop momenta.

TABLE I. Scale assignments and expansions of denominator factors corresponding to the regions in Figs. 2(b)–2(l).

(b)	$k, q, l, r \sim m_b$	$D_2 \to (q-r)^2$, $D_3 \to q^2$, $D_4 \to (q+l)^2$, $D_5 \to (q+l-r)^2$
(c)	$q-r \sim m_c$, $k, q, l \sim m_b$	$D_3 \to q^2$, $D_4 \to (q+l)^2$, $D_5 \to l^2$, $D_6 \to q^2$, $D_9 \to (p+k)^2$
(d)	$q \sim m_c$, $k, l, r \sim m_b$	$D_2 \to r^2$, $D_4 \to l^2$, $D_5 \to (l-r)^2$, $D_9 \to (p+k+r)^2$
(e)	$q+l \sim m_c$, $k, l, r \sim m_b$	$D_2 \to (l+r)^2$, $D_3 \to l^2$, $D_5 \to r^2$, $D_9 \to (p+k+l-r)^2$
(f)	$l+q-r \sim m_c$, $k, q, l \sim m_b$	$D_2 \to l^2$, $D_3 \to q^2$, $D_4 \to (l+q)^2$, $D_6 \to (l+q)^2$, $D_9 \to (p+l+k)^2$
(g)	$r, q \sim m_c$, $k, l \sim m_b$	$D_4 \to l^2$, $D_5 \to l^2$, $D_9 \to (p+k)^2$
(h)	$q-r, q+l \sim m_c$, $k, l \sim m_b$	$D_3 \to l^2$, $D_5 \to l^2$, $D_6 \to l^2$, $D_9 \to (p+k)^2$
(i)	$q, l \sim m_c$, $k, r \sim m_b$	$D_2 \to r^2$, $D_5 \to r^2$, $D_9 \to (p+k+r)^2$, $D_8 \to (2pl + i0)$
(j)	$q, l+q-r \sim m_c$, $k, l \sim m_b$	$D_2 \to l^2$, $D_4 \to l^2$, $D_6 \to l^2$, $D_9 \to (p+k+l)^2$
(k)	$r, q+l \sim m_c$, $k, l \sim m_b$	$D_2 \to l^2$, $D_3 \to l^2$, $D_9 \to (p+k+l)^2$
(l)	$l, q, r \sim m_c$, $k \sim m_b$	$D_9 \to (p+k)^2$, $D_8 \to (2pl + i0)$

One technical difficulty in this procedure is disentangling the products of loop momenta in the numerator, naturally appearing in the expansion. In the most difficult cases, we employed the method of Ref. [10], leading to a huge number of terms at higher orders in ρ. With intermediate expression size reaching hundred gigabytes, some tuning of the hardware and the computer algebra system [11] was required.

The three-loop eikonal integrals in region (l) correspond to topologies studied in Ref. [12]. Using the integration-by-parts identities [13–15], we reduce the expressions to a few "master integrals" found in Refs. [12,16], and a previously unpublished integral calculated by V. A. Smirnov, Eq. (C1).

The four-loop "all-hard" case (b) here is the most challenging. To expand X_2 to $\mathcal{O}(\rho^7)$, an implementation of algorithm [15] was running for several weeks. Finally, all diagrams were reduced to the 33 master integrals. Their evaluation was the biggest challenge of this work.

IV. EVALUATION OF FOUR-LOOP MASTER INTEGRALS

The results for master integrals given in [3] are sufficient to obtain $\mathcal{O}(\rho^0)$ and $\mathcal{O}(\rho^2)$ terms of X_2. However, in order to find the following $\mathcal{O}(\rho^4)$ contribution, many integrals need to be expanded further. In [3], the initial terms of that expansion were obtained in a series of steps. First, some of the internal lines of the diagram, representing a given master integral, were assigned a mass M much larger than the mass of the external particle m. Next, the diagram was expanded in m/M using a similar approach as described in the previous section; several terms of that expansion were obtained in each order in ϵ. Finally, and most nontrivial, a pattern in that expansion was recognized and the expansion was now summed analytically. The value of the result at $M = m$ gave the desired value of the integral.

In higher orders in ϵ, the recognition of the expansion pattern may be very difficult. Instead, we evaluate these integrals using the method of differential equations [17]. We start by choosing a few artificial double-scale topologies, related in some limit to the needed integrals. We illustrate this approach with the topology shown in Fig. 3. It involves an artificial mass $\sqrt{1/x}$, and in the on shell limit $x \to 1$ reproduces the topology needed for the first diagram shown in Fig. 1 (where we also introduce the loop factor $\mathcal{F} = \frac{\Gamma(1+\epsilon)}{(4\pi)^{D/2}}$).

This function is chosen due to several reasons. First, if $0 < x \le 1$, the cuts are the same as in the on shell limit, and we may discard the real part in all calculations. Second, large mass expansion to a few orders in x and ϵ is relatively simple [3]. And third, the associated differential equations have a structure convenient for an iterative solution; this property will be explained later.

This topology has 40 master integrals. Derivative of any such integral can be recast in terms of integrals with shifted indices,

$$\frac{\partial}{\partial x} I(a_1, \ldots, a_9; x) = \frac{a_5}{x^2} I(a_1, \ldots, a_5 + 1, \ldots) + \frac{a_6}{x^2} I(a_1, \ldots, a_6 + 1, \ldots), \qquad (7)$$

generating a system of 40 differential equations. It can be split into independent subsystems of at most four equations, where the solution of one system enters the right-hand side of the following one.

For example, consider functions $f(x, \epsilon) = I(0, 1, 1, 0, 1, 0, 0, 1, 0; x)$, $g(x, \epsilon) = I(-1, 1, 1, 0, 1, 0, 0, 1, 0; x)$, and $h(x, \epsilon) = I(0, 1, 1, -1, 1, 0, 0, 1, 0; x)$, entering a particularly simple system of relations

$$\begin{aligned}
f' &= \frac{4x - 5 + \epsilon(7 - 6x)}{2x(1-x)} f + \frac{9 - 11\epsilon}{2(1-x)} g + \frac{3\epsilon - 3}{2(1-x)} h, \\
g' &= \frac{1 - \epsilon}{2x(1-x)} f - \frac{8 + x - \epsilon(10 + x)}{2x(1-x)} g + \frac{3 - 3\epsilon}{2(1-x)} h, \\
h' &= \frac{1 - \epsilon}{2x^2} f + \frac{\epsilon - 1}{2x} g + \frac{3\epsilon - 3}{2x} h. \qquad (8)
\end{aligned}$$

We solve this system with respect to derivatives of f, and expand $f(x, \epsilon) = \frac{1}{\epsilon} f_{-1}(x) + f_0(x) + \epsilon f_1(x) + \ldots$. Finally, the differential equations for f_i become

$$\begin{aligned}
&f_i''' + \frac{9 - 6x}{x(1-x)} f_i'' + \frac{18 - 6x}{x^2(1-x)} f_i' + \frac{6}{x^3(1-x)} f_i = R_i, \\
&R_{-1} = 0, \\
&R_0 = \frac{6x - 9}{x(1-x)} f_{-1}'' + \frac{6x - 18}{x^2(1-x)} f_{-1}' + \frac{31}{x^3(1-x)} f_{-1}, \ldots. \qquad (9)
\end{aligned}$$

The three solutions of the homogeneous equation (with $R_i = 0$) can be guessed: $1/x$, $1/x^2$, and $(1 - x^2(x + 6) + 6x(1 + x)\ln x)/x^3$. Euler's formula allows then to solve the inhomogeneous equations. To fix the three integration

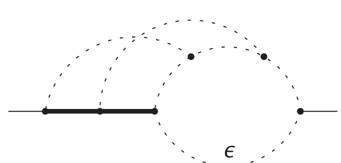

$$I(a_1, \ldots, a_9; x) = \frac{1}{\pi \mathcal{F}^4} \mathrm{Im} \int \frac{[d^D k][d^D q][d^D r] \quad D_9^{-a_9}}{D_1^{a_1+\epsilon} D_2^{a_2} D_3^{a_3} D_4^{a_4} D_5^{a_5} D_6^{a_6} D_7^{a_7} D_8^{a_8}},$$

$$p^2 = -1, D_1 = k^2, \; D_2 = (k+p)^2, \; D_3 = (k+q+p)^2,$$

$$D_4 = (k+q+r+p)^2, \; D_5 = (q+r+p)^2 + 1/x,$$

$$D_6 = (r+p)^2 + 1/x, \; D_7 = q^2, \; D_8 = r^2, \; D_9 = 2qp.$$

FIG. 3. Auxiliary double-scale topology. Thick lines represent mass $\sqrt{1/x}$, thin lines represent unit mass propagators, and ϵ labels a denominator raised to a noninteger power.

constants, we use the large mass expansion

$$f(x,\epsilon) = -\frac{1}{4x\epsilon} + \frac{1}{24} - \frac{15 + 4\ln x}{8x} + \epsilon\left(\frac{2\pi^2 - 145 - 60\ln x - 8\ln^2 x}{16x} + \frac{1}{4} + \frac{\ln x}{12} + \frac{x}{144} + \frac{x^2}{1440} + \ldots\right) + \ldots. \tag{10}$$

The general solution for f_i is expanded and matched to this series to find suitable constants. Finally, we obtain x-dependent solutions:

$$f_{-1} = -\frac{1}{4x}, \qquad f_0 = \frac{1}{24} - \frac{15 + 4\ln x}{8x},$$
$$f_1 = \frac{19}{36} + \frac{1}{12x^2} + \frac{6\pi^2 - 373}{48x} + \frac{H(0;x)(x-45)}{12x} + \frac{H(1;x)(x^3 + 9x^2 - 9x - 1)}{12x^3} - \frac{H(0,1;x)}{2x^2} - \frac{H(0,0;x)}{x}, \ldots \tag{11}$$

Because of the fact that the answers can be expressed in terms of harmonic polylogarithms (HPLs) $H(\ldots;x)$ [18], the expansion can be continued as long as CPU resources allow. (More accurately, this procedure works as long as the solutions of the homogeneous equation, as well as their inverse Wronskian and minors of Wronski matrix depend on x in the denominators only through factors x and $1 \pm x$, and numerators contain HPLs and polynomials. This allows to solve the inhomogeneous equation in terms of HPLs.) Taking the limit $x \to 1$, we obtain the required on shell integral.

One integral of the topology shown in Fig. 3, $u(x,\epsilon) = I(0,1,1,1,1,1,1,1,0;x)$, presents an additional difficulty. Its x-dependent expression starts at $\mathcal{O}(\epsilon)$ and logarithmically diverges at $x = 1$. To find that integral, we evaluated instead the infrared-safe function $I(1,1,1,1,1,1,1,1,-1;x)$, took the on shell limit and then reduced to $u(1,\epsilon)$. This lead to finite $\mathcal{O}(\epsilon^0)$ and $\mathcal{O}(\epsilon)$ expressions: $u(1,\epsilon) = -\frac{4\pi^4}{135} - \epsilon(\frac{95\zeta_5}{6} + \frac{13\pi^2\zeta_3}{18} + \frac{8\pi^4}{135})$. As a trade off, other integrals were needed to a higher order in ϵ, involving harmonic polylogarithms up to weight six.

An important tool was the software package HPL [19] and additional software for the series expansion of harmonic polylogarithms was developed [20]. As an independent check, we used numerical integration of the Mellin-Barnes representation of some integrals [21].

V. RESULTS AND SUMMARY

The rather lengthy expressions for X_L, X_H, X_C, X_A, and X_{NA} calculated through $\mathcal{O}(\rho^7)$ are presented in Appendix A. Their features, such as the logarithms and even and odd powers of ρ, together with physics consequences, have been discussed in [1]. Here we would like to illustrate the convergence of the expansion. To this end, Fig. 4 shows the plots of X_i as functions of ρ, in two versions: solid lines show all known terms while dashed lines are obtained by leaving out the last known power of ρ. We see that the convergence is excellent up to at least $\rho = 0.3$ of interest in this study.

In addition to the integrated decay rate, precision fits to experimental data are done for the moments of the lepton energy E_l and the hadronic-system energy E_h distributions in the rest frame of the b quark, with the goal of accurately measuring several parameters including $|V_{cb}|$, m_b, and the Wilson coefficient of nonperturbative operators. Thus, QCD corrections to those moments are also of interest. These corrections are defined by

$$\int \left(\frac{E_l}{m_b}\right)^n d\Gamma = \Gamma_0\left[L_0^{(n)} + C_F\frac{\alpha_s}{\pi}L_1^{(n)} + C_F\left(\frac{\alpha_s}{\pi}\right)^2 L_2^{(n)}\right], \tag{12}$$

and similarly for the moments of E_h, described by coefficients $H_j^{(n)}$; the average is taken over the whole phase space of decay products. One-loop spectra are known exactly [22], and Fig. 5 presents NNLO corrections $L_2^{(1,2)}$ and $H_2^{(1,2)}$. In [1], we discussed how the experimental cuts

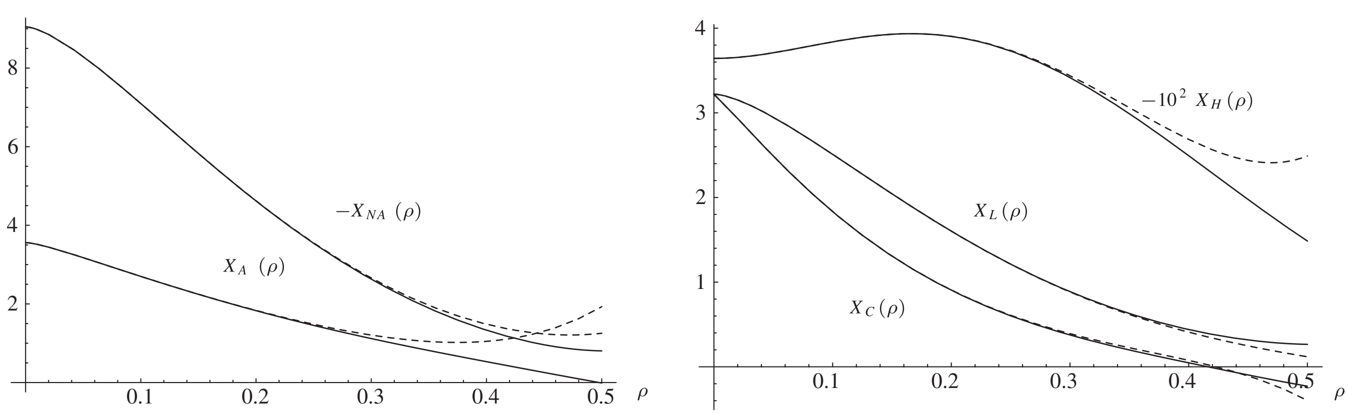

FIG. 4. Mass-dependent corrections to X_2 of Eq. (1).

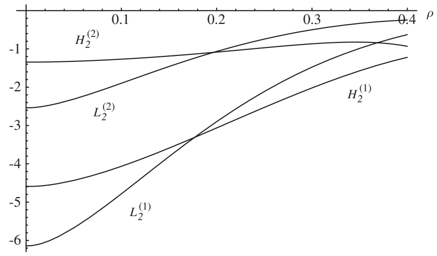

FIG. 5. First two moments of lepton and hadron energy distributions.

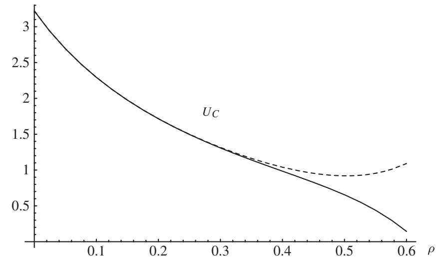

FIG. 6. Charm quark contribution to semileptonic $b \to u$ decays.

can be approximately modeled by the analytical calculation. Finally, we present the analytical results for U_C [Eq. (A6) and Fig. 6], an analogue of X_C in Eq. (1), describing charm quark loop contribution to the process with a massless quark in the final state, $b \to u\ell\bar{\nu}$.

The same method can be used in the model in which chiral weak coupling of quarks, $\frac{ig_w}{2\sqrt{2}}\gamma_\mu(1-\gamma_5)$, are replaced with a pure vector vertex, $\frac{ig_w}{2}\gamma_\mu$. This is a useful toy model, e.g., for logarithmic resummation studies [23]. In parametrization similar to Eq. (1), the second-order components V_i are defined in Eqs. (B1)–(B7). We evaluated terms to $\mathcal{O}(\rho^5)$, and it is now easy to find more.

To summarize, in the process of this calculation, we checked and confirmed the massless limit of the $\mathcal{O}(\alpha_s^2)$ corrections [2–4]. We extended those results to several orders in the mass ratio of the final and initial quarks. To complete this task, additional terms of master integrals were required, and the differential-equation method was applied to compute them. Our results agree excellently with the numerical calculation [24]. An ultimate test of the convergence of the mass expansion will be a corresponding expansion around the opposite mass limit, $m_c \simeq m_b$. Work on this is in progress.

ACKNOWLEDGMENTS

We thank A. Davydychev, M. Dowling, M. Kalmykov, A. Kotikov, A. Penin, and J. Piclum for many helpful discussions. This work was supported by Science and Engineering Research Canada.

APPENDIX A: ANALYTICAL RESULTS

Here we present the components of the total decay rate evaluated to $\mathcal{O}(\rho^7)$. In the case of the b-quark loop contribution, X_H, Fig. 4 shows an extremum point around $\rho = 0.2$. This contrasts with the other contributions, that seem to be monotonous functions of ρ. In order to double check the convergence, also the $\mathcal{O}(\rho^8)$ term has been computed. The final results are

$$\begin{aligned} X_L = & -\frac{1009}{288} + \frac{8\zeta_3}{3} + \frac{77\pi^2}{216} + \left\{\frac{118}{3} - \frac{4\pi^2}{3} + \frac{52}{3}\ln\rho - 8\ln^2\rho\right\}\rho^2 + \left\{\frac{64\ln 2}{3} - \frac{112}{9} + \frac{32}{3}\ln\rho\right\}\pi^2\rho^3 \\ & + \left\{76\zeta_3 - \frac{5\pi^2}{3} - 33 + 52\ln^2\rho + \left(39 - \frac{16}{3}\pi^2\right)\ln\rho - 32\ln^3\rho\right\}\rho^4 + \left\{\frac{64\ln 2}{3} - \frac{1216}{45} + \frac{32}{3}\ln\rho\right\}\pi^2\rho^5 \\ & + \left\{\frac{344}{27} + \frac{28\pi^2}{27} - \frac{1564}{27}\ln\rho + 24\ln^2\rho\right\}\rho^6 + \frac{40}{21}\pi^2\rho^7, \end{aligned} \tag{A1}$$

$$\begin{aligned} X_C = & -\frac{1009}{288} + \frac{8\zeta_3}{3} + \frac{77\pi^2}{216} - \frac{5}{4}\pi^2\rho + \left\{\frac{145}{3} + \frac{16\pi^2}{3} + \frac{52}{3}\ln\rho - 8\ln^2\rho\right\}\rho^2 + \left\{\frac{569}{36} + \frac{64}{3}\ln\rho\right\}\pi^2\rho^3 \\ & + \left\{196\zeta_3 + \frac{\pi^2}{6} - \frac{4483}{36} + 44\ln^2\rho - 32\ln^3\rho + \left(\frac{599}{6} + \frac{74\pi^2}{3}\right)\ln\rho\right\}\rho^4 + \left\{\frac{50}{3}\ln\rho - \frac{172}{9}\right\}\pi^2\rho^5 \\ & - \left\{\frac{33\,982}{225} + \frac{232\pi^2}{27} - \frac{11\,836}{135}\ln\rho + \frac{64}{9}\ln^2\rho\right\}\rho^6 + \left\{\frac{44}{3} + 18\ln\rho\right\}\pi^2\rho^7, \end{aligned} \tag{A2}$$

$$\begin{aligned} X_H = & \frac{16\,987}{576} - \frac{64\zeta_3}{3} - \frac{85\pi^2}{216} + \left\{\frac{8\pi^2}{3} - \frac{1198}{45}\right\}\rho^2 + \left\{\frac{156\,901\,877}{2\,116\,800} - \frac{11\pi^2}{18} - 64\zeta_3 - \left(\frac{186\,689}{2520} - \frac{20\pi^2}{3}\right)\ln\rho\right\}\rho^4 \\ & + \left\{\frac{189\,825\,233}{7\,144\,200} - \frac{52\pi^2}{27} - \frac{181\,627}{14\,175}\ln\rho + \frac{16}{5}\ln^2\rho\right\}\rho^6 + \left\{\frac{629\,309}{1\,403\,325} - \frac{4\zeta_3}{3} + \frac{19\pi^2}{72} - \left(\frac{4741}{9072} + \frac{\pi^2}{9}\right)\ln\rho\right\}\rho^8, \end{aligned} \tag{A3}$$

$$X_A = \frac{11\,047}{2592} - \frac{223\zeta_3}{36} - \frac{515\pi^2}{81} + \frac{53\pi^2\ln 2}{6} + \frac{67\pi^4}{720} + \left\{\frac{497\pi^2}{108} - \frac{2089}{8} + 86\zeta_3 - 8\pi^2\ln 2 + \frac{121\pi^4}{540} - 105\ln\rho - 36\ln^2\rho\right\}\rho^2 + \left\{\frac{752}{9} - \frac{112\pi}{3}\right\}\pi^2\rho^3 + \left\{\frac{16\,586}{27} - \frac{1139\pi^2}{24} - \frac{795\zeta_3}{2} + \frac{415\pi^2\zeta_3}{3} + 13\pi^2\ln 2 - 96\,\mathrm{Li}_4\frac{1}{2} - 8\pi^2\ln^2 2 - 4\ln^4 2 - 144\ln^3\rho - \left(\frac{19\,459}{18} + \frac{71\pi^2}{3} - 246\zeta_3 + 60\pi^2\ln 2 - \frac{40\pi^4}{3}\right)\ln\rho - \frac{349\pi^4}{72} + (99 + 4\pi^2)\ln^2\rho + 935\zeta_5\right\}\rho^4 + \left\{\frac{67\,448}{675} - \frac{776\pi}{15} + 160\ln\rho\right\}\pi^2\rho^5 + \left\{\frac{4859\zeta_3}{12} - \frac{1732}{9} - \frac{14\,921\pi^2}{216} + \frac{89\pi^2\ln 2}{6} - \frac{10\pi^4}{3} + \left(\frac{1862}{9} - \frac{34\pi^2}{3}\right)\ln^2\rho - \left(\frac{3635}{18} + 136\zeta_3 - \frac{833\pi^2}{18}\right)\ln\rho\right\}\rho^6 + \left\{\frac{86\pi}{7} - \frac{469\,304}{11\,025} + \frac{1376}{45}\ln\rho\right\}\pi^2\rho^7, \tag{A4}$$

$$X_{NA} = -\frac{X_A}{2} + \frac{19\,669}{1152} - \frac{70\pi^2}{27} + \frac{7\pi^4}{60} - \frac{101\zeta_3}{12} + \left\{\frac{11\pi^4}{18} - \frac{1813}{8} - \frac{19\pi^2}{6} - \frac{685}{6}\ln\rho + 4\ln^2\rho\right\}\rho^2 + \left\{\frac{2044}{9} - \frac{1136\ln 2}{3} - \frac{124}{3}\ln\rho\right\}\pi^2\rho^3 + \left\{\frac{8947}{32} - \frac{103\pi^2}{12} + \frac{2\pi^4}{45} + 200\zeta_5 - \frac{705\zeta_3}{2} + \frac{100\pi^2\zeta_3}{3} + \left(84\zeta_3 - \frac{1049}{2} - \frac{161\pi^2}{6} + \frac{10\pi^4}{3}\right)\ln\rho + \left(7\pi^2 - \frac{271}{2}\right)\ln^2\rho + 16\ln^3\rho\right\}\rho^4 + \left\{\frac{58\,024}{225} - \frac{1136\ln 2}{3} - \frac{292}{15}\ln\rho\right\}\rho^5\pi^2 + \left\{\frac{269\,297}{1296} + \frac{2303\pi^2}{216} - \frac{\pi^4}{2} - 24\zeta_3 + \left(12\zeta_3 - \frac{2441}{72} - \frac{17\pi^2}{3}\right)\ln\rho + \left(\frac{229}{9} + \pi^2\right)\ln^2\rho\right\}\rho^6 - \left\{\frac{242\,554}{33\,075} + \frac{256}{315}\ln\rho\right\}\pi^2\rho^7. \tag{A5}$$

The charm quark contribution to $b \to u\ell\bar{\nu}$ decays through $\mathcal{O}(\rho^7)$ is:

$$U_C = -\frac{1009}{288} + \frac{8\zeta_3}{3} + \frac{77\pi^2}{216} - \frac{5}{4}\pi^2\rho + \left\{21 + \frac{8\pi^2}{3}\right\}\rho^2 + \left\{\frac{64\ln 2}{3} - \frac{95}{36} + \frac{32}{3}\ln\rho\right\}\pi^2\rho^3 + \left\{48\zeta_3 - \frac{4375}{36} - \frac{25\pi^2}{6} + \left(\frac{365}{6} + 6\pi^2\right)\ln\rho - 8\ln^2\rho\right\}\rho^4 - \frac{112}{15}\pi^2\rho^5 + \left\{\frac{7804}{675} + \frac{64\pi^2}{27} + \frac{8}{5}\ln\rho - \frac{64}{9}\ln^2\rho\right\}\rho^6 - \frac{24}{7}\pi^2\rho^7. \tag{A6}$$

APPENDIX B: A VECTOR MODEL

As a by-product of this project, for the purpose of comparisons with [23], we have determined $\mathcal{O}(\alpha_s^2)$ corrections to the decay rate in a model where the W boson has only a vector, and no axial vector, coupling to fermions. That is, its interaction vertex is obtained from the standard $(V - A)$ one by the substitution $\frac{ig_w}{2\sqrt{2}}\gamma_\mu(1-\gamma_5) \to \frac{ig_w}{2}\gamma_\mu$. The results for this model are parametrized in analogy with Eqs. (1)–(4), with replacements $X_i \to V_i$. Results for the tree-level and first-order corrections, expanded through $\mathcal{O}(\rho^5)$, are

$$V_0 = 1 - 2\rho - 8\rho^2 - \{18 + 24\ln\rho\}\rho^3 - 24\rho^4\ln\rho + \{18 - 24\ln\rho\}\rho^5, \tag{B1}$$

$$V_1 = \frac{25}{8} - \frac{\pi^2}{2} + \{\pi^2 - 10 - 3\ln\rho\}\rho - \{34 + 24\ln\rho\}\rho^2 + \{13\pi^2 - 90 - 81\ln\rho - 36\ln^2\rho\}\rho^3 + \left\{24\pi^2 - \frac{273}{2} + 36\ln\rho - 72\ln^2\rho\right\}\rho^4 + \left\{13\pi^2 - \frac{369}{2} + 135\ln\rho - 72\ln^2\rho\right\}\rho^5. \tag{B2}$$

The difference with the standard decay is seen already at the tree level: odd powers of ρ are present in V_0, while in the $V - A$ decay they appeared only in the first-order corrections. The reason for this is a contribution of a four-quark operator, as discussed in [1,23]. In the $V - A$ decay, a similar operator contributes only through its $\mathcal{O}(\alpha_s)$ matrix element. As a result, the second-order corrections in the vector case are even more complicated than in the $V - A$ decay. They read

$$
\begin{aligned}
V_A &= \frac{11\,047}{2592} - \frac{223\zeta_3}{36} - \frac{515\pi^2}{81} + \frac{53\pi^2\ln 2}{6} + \frac{67\pi^4}{720} + \bigg\{\frac{1997\pi^2}{648} - \frac{81\,149}{1944} + \frac{317\zeta_3}{18} - \frac{\pi^2\ln 2}{3} - \frac{211\pi^4}{1080} - \frac{9}{4}\ln^2\rho \\
&\quad + \left(\frac{3\pi^2}{2} - \frac{123}{8}\right)\ln\rho\bigg\}\rho + \bigg\{\frac{497\pi^2}{108} - \frac{2089}{8} + 86\zeta_3 - 8\pi^2\ln 2 + \frac{121\pi^4}{540} - 105\ln\rho - 36\ln^2\rho\bigg\}\rho^2 \\
&\quad + \bigg\{\frac{4667\pi^2}{72} - \frac{16\,943}{36} + 561\zeta_5 - \frac{37\zeta_3}{2} - 48\,\mathrm{Li}_4\frac{1}{2} - 2\ln^4 2 + 83\pi^2\zeta_3 - 17\pi^2\ln 2 + \bigg(8\pi^4 + 328\zeta_3 + \frac{125\pi^2}{6} \\
&\quad - \frac{50\,969}{72} - 64\pi^2\ln 2\bigg)\ln\rho - \frac{112\pi^3}{3} - 8\pi^2\ln^2 2 + \frac{449\pi^4}{120} + \left(12\pi^2 - \frac{747}{4}\right)\ln^2\rho - 63\ln^3\rho\bigg\}\rho^3 \\
&\quad + \bigg\{\frac{16\,586}{27} + \frac{13\,223\pi^2}{72} - 96\,\mathrm{Li}_4\frac{1}{2} + 13\pi^2\ln 2 - \frac{795\zeta_3}{2} + \frac{415\pi^2\zeta_3}{3} + 935\zeta_5 - 4\ln^4 2 - 8\pi^2\ln^2 2 - \frac{304\pi^3}{3} \\
&\quad - \frac{349\pi^4}{72} - 144\ln^3\rho + (99 + 4\pi^2)\ln^2\rho + \left(\frac{40\pi^4}{3} - \frac{19\,459}{18} + 246\zeta_3 + \frac{361\pi^2}{3} - 60\pi^2\ln 2\right)\ln\rho\bigg\}\rho^4 \\
&\quad + \bigg\{\frac{14\,036}{27} + 561\zeta_5 + \frac{109\zeta_3}{2} - 24\,\mathrm{Li}_4\frac{1}{2} - \ln^4 2 + \frac{264\,109\pi^2}{5400} + 83\pi^2\zeta_3 + 41\pi^2\ln 2 + \bigg(81\zeta_3 - \frac{8456}{9} + \frac{401\pi^2}{2} \\
&\quad - 66\pi^2\ln 2 + 8\pi^4\bigg)\ln\rho + \left(\frac{1395}{4} - 8\pi^2\right)\ln^2\rho - 141\ln^3\rho - 8\pi^2\ln^2 2 - \frac{776\pi^3}{15} - \frac{1093\pi^4}{90}\bigg\}\rho^5,
\end{aligned}
\tag{B3}
$$

$$
\begin{aligned}
V_{NA} &= -\frac{V_A}{2} + \frac{19\,669}{1152} - \frac{70\pi^2}{27} + \frac{7\pi^4}{60} - \frac{101\zeta_3}{12} + \bigg\{\frac{337\pi^2}{54} - \frac{8707}{144} + \frac{107\zeta_3}{6} - \frac{7\pi^4}{30} + \left(\frac{3\pi^2}{4} - \frac{739}{48}\right)\ln\rho + \frac{13\ln^2\rho}{8}\bigg\}\rho \\
&\quad + \bigg\{\frac{11\pi^4}{18} - \frac{1813}{8} - \frac{19\pi^2}{6} - \frac{685}{6}\ln\rho + 4\ln^2\rho\bigg\}\rho^2 + \bigg\{\frac{7309\pi^2}{36} - \frac{8039}{16} + \frac{47\pi^4}{30} - \frac{1136\pi^2\ln 2}{3} - \frac{333\zeta_3}{2} + 20\pi^2\zeta_3 \\
&\quad + 120\zeta_5 + \left(36\zeta_3 - \frac{6867}{16} - \frac{541\pi^2}{12} + 2\pi^4\right)\ln\rho + \left(3\pi^2 - \frac{893}{8}\right)\ln^2\rho + \frac{47}{2}\ln^3\rho\bigg\}\rho^3 + \bigg\{\frac{8947}{32} + \frac{5977\pi^2}{12} + \frac{2\pi^4}{45} \\
&\quad - \frac{2272\pi^2\ln 2}{3} - \frac{705\zeta_3}{2} + \frac{100\pi^2\zeta_3}{3} + 200\zeta_5 + \left(84\zeta_3 - \frac{1049}{2} - \frac{171\pi^2}{2} + \frac{10\pi^4}{3}\right)\ln\rho + \left(7\pi^2 - \frac{271}{2}\right)\ln^2\rho \\
&\quad + 16\ln^3\rho\bigg\}\rho^4 + \bigg\{\frac{8313}{16} + \frac{518\,717\pi^2}{1800} - \frac{83\pi^4}{30} - \frac{1136\pi^2\ln 2}{3} - \frac{459\zeta_3}{2} + 20\pi^2\zeta_3 + 120\zeta_5 \\
&\quad + \left(72\zeta_3 - \frac{4737}{16} - \frac{2293\pi^2}{60} + 2\pi^4\right)\ln\rho + \left(6\pi^2 - \frac{871}{8}\right)\ln^2\rho + \frac{33}{2}\ln^3\rho\bigg\}\rho^5
\end{aligned}
\tag{B4}
$$

$$
\begin{aligned}
V_L &= -\frac{1009}{288} + \frac{8\zeta_3}{3} + \frac{77\pi^2}{216} + \bigg\{\frac{215}{18} - \frac{16\zeta_3}{3} - \frac{43\pi^2}{54} + \frac{13}{6}\ln\rho - \ln^2\rho\bigg\}\rho + \bigg\{\frac{118}{3} - \frac{4\pi^2}{3} + \frac{52}{3}\ln\rho - 8\ln^2\rho\bigg\}\rho^2 \\
&\quad + \bigg\{\frac{163}{2} + 48\zeta_3 - \frac{293\pi^2}{18} + \left(\frac{93}{2} + \frac{20\pi^2}{3}\right)\ln\rho - \ln^2\rho - 20\ln^3\rho + \frac{64\pi^2\ln 2}{3}\bigg\}\rho^3 + \bigg\{76\zeta_3 - 33 - \frac{133\pi^2}{3} \\
&\quad + (39 + 16\pi^2)\ln\rho + 52\ln^2\rho - 32\ln^3\rho + \frac{128\pi^2\ln 2}{3}\bigg\}\rho^4 + \bigg\{\frac{1}{2} + 36\zeta_3 - \frac{2417\pi^2}{90} + \frac{64\pi^2\ln 2}{3} \\
&\quad + \left(\frac{14\pi^2}{3} - \frac{195}{2}\right)\ln\rho + 109\ln^2\rho - 36\ln^3\rho\bigg\}\rho^5,
\end{aligned}
\tag{B5}
$$

$$
\begin{aligned}
V_H &= \frac{16\,987}{576} - \frac{64\zeta_3}{3} - \frac{85\pi^2}{216} + \bigg\{\frac{35\pi^2}{54} - \frac{4109}{216} + \frac{32\zeta_3}{3}\bigg\}\rho + \bigg\{\frac{8\pi^2}{3} - \frac{1198}{45}\bigg\}\rho^2 + \bigg\{\frac{9\pi^2}{2} - 16\zeta_3 - \frac{30\,043}{1080} \\
&\quad + \left(\frac{20\pi^2}{3} - \frac{1193}{18}\right)\ln\rho\bigg\}\rho^3 + \bigg\{\frac{156\,901\,877}{2\,116\,800} - \frac{11\pi^2}{18} - 64\zeta_3 + \left(\frac{20\pi^2}{3} - \frac{186\,689}{2520}\right)\ln\rho\bigg\}\rho^4 + \bigg\{\frac{24\,416\,711}{352\,800} \\
&\quad - 24\zeta_3 - \frac{9\pi^2}{2} + \left(6\pi^2 - \frac{9883}{140}\right)\ln\rho\bigg\}\rho^5,
\end{aligned}
\tag{B6}
$$

$$V_C = -\frac{1009}{288} + \frac{8}{3}\zeta_3 + \frac{77}{216}\pi^2 + \left\{\frac{94}{9} - \frac{16\zeta_3}{3} - \frac{167\pi^2}{108} + \frac{13}{6}\ln\rho - \ln^2\rho\right\}\rho + \left\{\frac{145}{3} + \frac{22\pi^2}{3} + \frac{52}{3}\ln\rho - 8\ln^2\rho\right\}\rho^2 + \left\{68 + 120\zeta_3 - 20\ln^3\rho + \frac{1061\pi^2}{36} + \left(\frac{129}{2} + \frac{106\pi^2}{3}\right)\ln\rho - \ln^2\rho\right\}\rho^3 + \left\{196\zeta_3 - \frac{4483}{36} - \frac{121\pi^2}{18} + \left(\frac{599}{6} + \frac{158\pi^2}{3}\right)\ln\rho + 44\ln^2\rho - 32\ln^3\rho\right\}\rho^4 + \left\{200\zeta_3 - \frac{20\,557}{72} - \frac{185\pi^2}{6} + \left(\frac{98\pi^2}{3} + \frac{686}{3}\right)\ln\rho - 36\ln^2\rho - 12\ln^3\rho\right\}\rho^5. \tag{B7}$$

APPENDIX C: MASTER INTEGRALS

In this appendix, we collect new results for master integrals that were obtained in this project.

For the three-loop integrals needed for the factorized diagrams of the type shown in Fig. 2(l), the $\mathcal{O}(\epsilon)$ term of the integral J_3 of Ref. [12] was needed. It was privately communicated to us by V. A. Smirnov,

$$\frac{J_3}{\pi^2\mathcal{F}^3} = -\frac{32}{3} + \left(\frac{256\ln 2}{3} - \frac{448}{3} - \frac{64\pi}{3}\right)\epsilon, \qquad \mathcal{F} \equiv \frac{\Gamma(1+\epsilon)}{(4\pi)^{D/2}}. \tag{C1}$$

For the unfactorized four-loop diagrams in Fig. 2(b), the master integrals have already been classified and largely evaluated in Ref. [3]. Using the approach described in

TABLE II. Additional terms for master integrals of Ref. [3], as defined in Eq. (C2).

$\Delta_A(1,1,1,1,0,1,1,1,1,1,0)$	$55\zeta_5 - \frac{2\pi^4}{9} - \frac{13\pi^2\zeta_3}{2} + \epsilon(\frac{143\pi^6}{3240} - \frac{2\pi^4}{3} - 26\pi^2\zeta_3 - 51\zeta_3^2 + 220\zeta_5)$
$\Delta_A(1,1,1,0,1,0,1,1,1,0,0)$	$\epsilon^2(\frac{7945\pi^2}{48} - \frac{119\,727}{32} + \frac{269\pi^4}{72} + \frac{3185\zeta_3}{4} - \frac{49\pi^2\zeta_3}{3} + 279\zeta_5)$
$\Delta_A(1,0,1,1,0,1,0,1,0,1,0)$	$\epsilon^3(\frac{2\,515\,231}{1944} - \frac{101\,531\pi^2}{2592} - \frac{1309\pi^4}{180} - \frac{35\,951\zeta_3}{72} - \frac{7\pi^2\zeta_3}{3} - \frac{779\zeta_5}{2})$
$\Delta_A(1,1,1,1,0,1,0,1,0,1,0)$	$\epsilon^2(\frac{14\,437}{16} + \frac{169\pi^2}{16} + \frac{37\pi^4}{90} + \frac{5\zeta_3}{4} - 41\zeta_5)$
$\Delta_A(1,0,1,0,1,1,1,0,1,0,0)$	$\epsilon^3(\frac{51\,175\,105}{15\,552} - \frac{238\,819\pi^2}{2592} - \frac{3149\pi^4}{360} - \frac{54\,895\zeta_3}{72} + \frac{43\pi^2\zeta_3}{3} - \frac{1243\zeta_5}{2})$
$\Delta_A(1,1,1,0,1,1,1,0,1,0,0)$	$\epsilon^2(\frac{3587\pi^2}{48} - \frac{64177}{32} + \frac{367\pi^4}{180} + \frac{1245\zeta_3}{4} - \frac{4\pi^2\zeta_3}{3} + 59\zeta_5)$
$\Delta_A(1,0,1,1,1,1,0,0,1,1,0)$	$\epsilon^2(\frac{493\pi^2}{8} - \frac{119\,727}{32} + \frac{161\pi^4}{15} + 600\zeta_3 - \frac{20\pi^2\zeta_3}{3} + 1092\zeta_5)$
$\Delta_A(1,0,1,1,0,1,1,1,1,0,0)$	$\epsilon^2(\frac{3331\pi^4}{360} - \frac{147\,441}{64} - \frac{149\pi^2}{16} + \frac{1123\zeta_3}{4} + \frac{19\pi^2\zeta_3}{3} + 759\zeta_5)$
$\Delta_A(1,1,1,0,0,1,1,1,1,0,0)$	$\epsilon^2(\frac{4763\pi^2}{48} - \frac{38\,519}{16} + \frac{125\pi^4}{24} + \frac{2145\zeta_3}{4} - \frac{101\pi^2\zeta_3}{3} + 563\zeta_5)$
$\Delta_B(1,1,1,1,1,1,1,1,1,1,1)$	$\frac{1045\zeta_5}{32} - \frac{17\pi^4}{360} - \frac{77\pi^2\zeta_3}{32}$
$\Delta_B(1,1,1,1,1,1,0,1,1,1,0)$	$-\frac{17\pi^4}{60} - \frac{79\pi^2\zeta_3}{48} - \frac{355\zeta_5}{16}$
$\Delta_B(1,0,1,0,1,1,1,0,1,1,0)$	$\epsilon^3(72\pi^2 - \frac{124\,763}{32} + \frac{793\pi^4}{60} + \frac{1961\zeta_3}{2} - \frac{43\pi^2\zeta_3}{3} + 814\zeta_5)$
$\Delta_B(1,0,1,0,1,1,1,0,1,1,0)$	$\epsilon(\frac{1391}{2} - \frac{58\pi^2}{3} - \frac{9\pi^4}{20} - 68\zeta_3 + \pi^2\zeta_3 - 27\zeta_5)$
$\Delta_B(1,1,1,0,1,0,1,1,1,1,0)$	$\epsilon^2(2172 - \frac{317\pi^2}{6} - \frac{401\pi^4}{90} - 472\zeta_3 + \frac{25\pi^2\zeta_3}{3} - 232\zeta_5)$
$\Delta_B(1,1,1,0,1,1,1,0,1,0,0)$	$\epsilon(24A_4 + 6A_5 - \frac{\ln^5 2}{20} - 6\pi^2\ln 2 + \ln^4 2 - \frac{49\pi^4}{180} + \frac{19\pi^4\ln 2}{80} + 15\zeta_3 - \frac{51\pi^2\zeta_3}{16} + \frac{299\zeta_5}{32})$
$\Delta_B(1,0,1,1,1,1,0,0,2,2,0)$	$\epsilon^2(\frac{\ln^5 2}{20} - 12A_4 - 6A_5 - \frac{\ln^4 2}{2} - \frac{33\pi^2}{2} - \pi^2\ln 2 - \frac{11\pi^4}{60} - \frac{19\pi^4\ln 2}{80} - \frac{199\zeta_3}{2} + \frac{173\pi^2\zeta_3}{16} + \frac{5057\zeta_5}{32})$ $+\epsilon^3(12A_4 - 12A_5 - 6A_6 - \frac{159H_6}{2} + \frac{\ln^4 2}{2} + \frac{\ln^5 2}{10} - \frac{\ln^6 2}{120} - \frac{131\pi^2}{2} + \frac{99A_4\pi^2}{2} - 17\pi^2\ln 2 + \frac{33\pi^2\ln^4 2}{16} - \frac{31\pi^4}{4}$ $- \frac{975\zeta_3}{2} + \frac{47\pi^2\zeta_3}{3} - \frac{19\pi^4\ln 2}{40} - \frac{311\pi^4\ln^2 2}{160} + \frac{51\pi^2\zeta_3\ln 2}{2} + \frac{7213\pi^6}{5040} + \frac{2177\zeta_3^2}{16} - \frac{1749\zeta_5}{16})$
$\Delta_C(1,0,1,1,1,0,0,1,1,1,0)$	$\epsilon(\frac{167\pi^2}{12} - \frac{10\,325}{32} - 4\pi^2\ln 2 + \frac{149\pi^4}{360} + 105\zeta_3)$
$\Delta_C(1,0,1,1,1,1,0,1,1,1,0)$	$\epsilon(113 - 48A_4 - 2\ln^4 2 + \frac{151\pi^2}{6} + 4\pi^2\ln 2 - \frac{13\pi^4}{60} + 14\zeta_3) + \epsilon^2(934 - 576A_4 - 480A_5 - 24\ln^4 2$ $+4\ln^5 2 + \frac{356\pi^2}{3} + 42\pi^2\ln 2 - 8\pi^2\ln^2 2 + \frac{8\pi^2\ln^3 2}{3} + \frac{5\pi^4}{72} - \frac{3\pi^4\ln 2}{2} + 24\zeta_3 - \frac{59\pi^2\zeta_3}{6} + \frac{913\zeta_5}{4})$
$\Delta_C(1,0,1,1,1,1,0,1,1,1,0)$	$\epsilon^2(\frac{131\,899}{64} - 92\pi^2\ln 2 + 192A_4 + 8\ln^4 2 + \frac{543\pi^2}{16} + 16\pi^2\ln^2 2 - \frac{99\pi^4}{40} + \frac{831\zeta_3}{4} + \pi^2\zeta_3 - 45\zeta_5)$
$\Delta_E(1,1,1,0,1,1,1,1,1,1,0)$	$\frac{13\pi^2\zeta_3}{3} - \frac{4\pi^4}{15} - 94\zeta_5 + \epsilon(\frac{52\pi^2\zeta_3}{3} - \frac{4\pi^4}{5} - \frac{217\pi^6}{1620} + 6\zeta_3^2 - 376\zeta_5)$
$\Delta_F(1,1,1,1,1,1,1,1,1,1,1)$	$\frac{\pi^4}{30} + \frac{221\pi^2\zeta_3}{48} - \frac{799\zeta_5}{16}$
$\Delta_F(1,1,1,1,1,1,1,0,1,1,0)$	$\frac{61\pi^2\zeta_3}{48} - \frac{37\pi^4}{180} - \frac{1019\zeta_5}{16}$
$\Delta_F(1,0,1,1,1,1,1,0,1,2,0)$	$-\epsilon(\frac{3\pi^4}{20} + \frac{107\pi^2\zeta_3}{48} + \frac{547\zeta_5}{16})$
$\Delta_F(1,1,1,1,0,1,1,0,1,1,0)$	$\epsilon(1031 - \frac{199\pi^2}{6} - \frac{209\pi^4}{180} - 163\zeta_3 + \frac{7\pi^2\zeta_3}{3} - 64\zeta_5)$
$\Delta_F(1,1,1,1,0,0,1,1,1,1,0)$	$\epsilon^2(\frac{253\pi^2}{2} - 2172 + \frac{407\pi^4}{90} + 899\zeta_3 - \frac{98\pi^2\zeta_3}{3} + 403\zeta_5) + \epsilon^3(\frac{2007\pi^2}{2} + \frac{547\pi^4}{18} - 17037$ $+ \frac{487\pi^6}{1134} + 5869\zeta_3 - 396\zeta_3^2 + 4433\zeta_5 - \frac{1078\pi^2\zeta_3}{3})$
$\Delta_F(1,1,1,1,1,1,0,0,1,1,0)$	$46A_4 - 30 + \frac{23\ln^4 2}{12} + \frac{7\pi^2}{6} - 2\pi^2\ln 2 - \frac{5\pi^2\ln^2 2}{3} - \frac{\pi^4}{9} + 24\zeta_3 + \epsilon(184A_4 - 272 + 46A_5 + \frac{23\ln^4 2}{3}$ $- \frac{23\ln^5 2}{60} + \frac{67\pi^2}{6} - 3\pi^2\ln 2 - \frac{73\pi^4}{360} - \frac{20\pi^2\ln^2 2}{3} + \frac{5\pi^2\ln^3 2}{9} - \frac{547\pi^4\ln 2}{360} + \frac{209\zeta_3}{2} - \frac{99\pi^2\zeta_3}{8} + \frac{3921\zeta_5}{16})$

Sec. IV, we obtained additional terms of their expansion in ϵ. To save space, we present here only those additional terms, using the notation of Ref. [3], in particular, Eqs. (5.7–11) of that paper. Instead of repeating here the long expressions already known, we define Δ_N, $N = A..F$, to denote the new terms. For any affected master integral, its improved value can be found as follows,

$$\mathrm{Im}[I_N(a_1, \ldots, a_{11})] \equiv \pi s^j (N_\epsilon)^4 [\text{terms already known} + \Delta_N(a_1, \ldots, a_{11})], \quad \text{(C2)}$$

where, as defined in Ref. [3], $N_\epsilon = \frac{\pi^2}{(\pi s)^\epsilon} \frac{\Gamma^2(1-\epsilon)\Gamma(1+\epsilon)}{\Gamma(1-2\epsilon)}$ and s denotes the square of the momentum flowing into the diagram. Its power j depends on the integral considered and, for each one, can be found in Ref. [3]. Table II shows the extra terms Δ_N.

We use the following notation for transcendental constants, $A_n = \mathrm{Li}_n \frac{1}{2}$, $n = 4..6$, and $s_6 = 0.987\,441\,4\ldots$. Here Li_n denotes polylogarithms [25], $\mathrm{Li}_n x = \sum_{i=1}^{\infty} \frac{x^i}{i^n}$, and $s_6 \equiv S_{-5,-1}(\infty)$ is certain harmonic sum [19,26].

[1] A. Pak and A. Czarnecki, Phys. Rev. Lett. **100**, 241807 (2008).

[2] T. van Ritbergen and R. G. Stuart, Phys. Rev. Lett. **82**, 488 (1999).

[3] T. van Ritbergen and R. G. Stuart, Nucl. Phys. **B564**, 343 (2000); M. Steinhauser and T. Seidensticker, Phys. Lett. B **467**, 271 (1999).

[4] T. van Ritbergen, Phys. Lett. B **454**, 353 (1999).

[5] Y. Nir, Phys. Lett. B **221**, 184 (1989).

[6] S. A. Larin, Phys. Lett. B **303**, 113 (1993).

[7] F. V. Tkachev, Sov. J. Part. Nucl. **25**, 649 (1994).

[8] V. A. Smirnov, Springer Tracts Mod. Phys. **177**, 1 (2002).

[9] A. Czarnecki and V. A. Smirnov, Phys. Lett. B **394**, 211 (1997).

[10] A. I. Davydychev and J. B. Tausk, Nucl. Phys. **B465**, 507 (1996).

[11] J. A. M. Vermaseren, arXiv:math-ph/0010025.

[12] A. G. Grozin, A. V. Smirnov, and V. A. Smirnov, J. High Energy Phys. 11 (2006) 022.

[13] F. V. Tkachev, Phys. Lett. **100B**, 65 (1981).

[14] K. G. Chetyrkin and F. V. Tkachev, Nucl. Phys. **B192**, 159 (1981).

[15] S. Laporta, Int. J. Mod. Phys. A **15**, 5087 (2000).

[16] A. G. Grozin, T. Huber, and D. Maitre, J. High Energy Phys. 07 (2007) 033.

[17] E. Remiddi, Nuovo Cimento Soc. Ital. Fis. A **110**, 1435 (1997).

[18] E. Remiddi and J. A. M. Vermaseren, Int. J. Mod. Phys. A **15**, 725 (2000).

[19] D. Maitre, Comput. Phys. Commun. **174**, 222 (2006).

[20] A. Pak and J. Piclum (work in progress).

[21] M. Czakon, Comput. Phys. Commun. **175**, 559 (2006).

[22] A. Czarnecki, M. Jezabek, and J. H. Kuhn, Nucl. Phys. **B351**, 70 (1991).

[23] C. W. Bauer, A. F. Falk, and M. E. Luke, Phys. Rev. D **54**, 2097 (1996).

[24] K. Melnikov, arXiv:0803.0951.

[25] L. Lewin, *Polylogarithms and Associated Functions* (North Holland, New York, 1981).

[26] J. A. M. Vermaseren, Int. J. Mod. Phys. A **14**, 2037 (1999).